

# Wavelets on the sphere

New methodologies and cosmological applications

Jason McEwen

<http://www.mrao.cam.ac.uk/~jdm57/>

DAMTP Cosmology Lunch :: June 2007

# Outline

- 1 Motivation
- 2 Wavelets on the sphere
  - History
  - Methodology I
  - Methodology II
  - Comparison
  - Fast algorithms
- 3 Wavelet steerability
  - Steerability
  - Morphological measures
- 4 Detecting the ISW effect
  - Background
  - Procedures
  - Data and simulations
  - Detections

# Outline

- 1 Motivation
- 2 Wavelets on the sphere
  - History
  - Methodology I
  - Methodology II
  - Comparison
  - Fast algorithms
- 3 Wavelet steerability
  - Steerability
  - Morphological measures
- 4 Detecting the ISW effect
  - Background
  - Procedures
  - Data and simulations
  - Detections

# What's the point?



Fourier (1807)



Haar (1909)

Morlet and Grossman (1981)

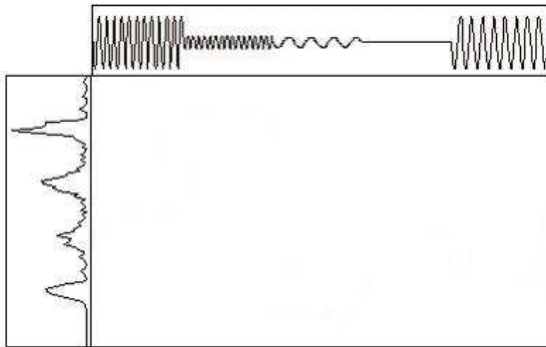


Figure: Fourier vs wavelet transform (image from <http://www.wavelet.org/tutorial/>)

# What's the point?



Fourier (1807)



Haar (1909)

Morlet and Grossman (1981)

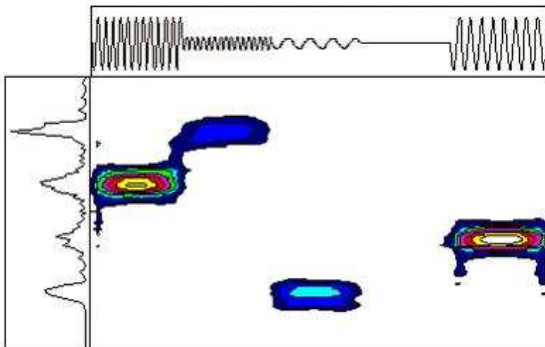


Figure: Fourier vs wavelet transform (image from <http://www.wavelet.org/tutorial/>)

# Wavelets in Euclidean space

- Decompose signal into wavelet basis

$$\mathcal{W}(a, b) = |a|^{-1/2} \int_{-\infty}^{\infty} dt f(t) \psi\left(\frac{t-b}{a}\right) = \langle f, \psi_{a,b} \rangle,$$

where  $\psi_{a,b} = |a|^{-1/2} \psi\left(\frac{t-b}{a}\right)$ .

- Synthesis signal from wavelet coefficients

$$f = C_{\psi}^{-1} \int_{-\infty}^{\infty} \int_{-\infty}^{\infty} \frac{da db}{a^2} \mathcal{W}(a, b) \psi_{a,b}.$$

- Admissibility condition to ensure perfect reconstruction

$$0 < C_{\psi} \equiv 2\pi \int_{-\infty}^{\infty} \frac{dk}{|k|} |\hat{\psi}(k)|^2 < \infty.$$

- Construct on sphere in analogous manner

# Outline

- 1 Motivation
- 2 Wavelets on the sphere
  - History
  - Methodology I
  - Methodology II
  - Comparison
  - Fast algorithms
- 3 Wavelet steerability
  - Steerability
  - Morphological measures
- 4 Detecting the ISW effect
  - Background
  - Procedures
  - Data and simulations
  - Detections

# History

- Discrete “**second generation**” wavelets on the sphere constructed through the lifting scheme (Schroder & Sweldens 1995 [17])
  - Avoids explicit definition of a dilation operator but may not lead to a stable basis and loose symmetry of sphere
- Extension of a **dilation operator** to the sphere non-trivial
- Various attempts (e.g. [6, 7, 8, 9, 14, 15, 18])
- Antoine and Vandergheynst 1998 (AV98) [2]  
→ **Methodology I**
- Sanz *et al.* 2006 (SHLA06) [16]; JDM, Hobson & Lasenby 2006 (MHL06) [10]  
→ **Methodology II**



# Methodology I: Overview

- Originally, construction derived entirely from group theoretical principles (AV98). However, in a recent work by Wiaux *et al.* 2005 [20] reintroduced independently of the original group theoretic formalism, in an equivalent, practical and self-consistent approach.
- Correspondence principle between spherical and Euclidean wavelets is developed, relating the concepts of planar Euclidean wavelets to spherical wavelets through a **stereographic projection**.
  - Stereographic projection is conformal, unitary and radial.
- Dilation** on sphere defined through stereographic projection operator; construct **wavelet basis** on sphere; **wavelet transform** on sphere projection onto this basis.
  - Mother wavelets must satisfy the appropriate **admissibility** criterion to ensure perfect reconstruction is possible.

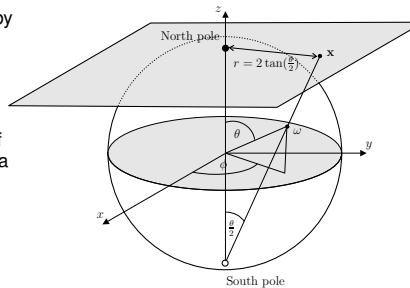


Figure: Stereographic projection

# Methodology I: Stereographic projection

- Stereographic projection operator is defined by  $\Pi : \omega \rightarrow \mathbf{x} = \Pi\omega = (r(\theta), \phi)$  where  $r = 2 \tan(\theta/2)$ ,  $\omega \equiv (\theta, \phi) \in \mathbb{S}^2$  and  $\mathbf{x} \in \mathbb{R}^2$  is a point in the plane, denoted here by the polar coordinates  $(r, \phi)$ . The inverse operator is  $\Pi^{-1} : \mathbf{x} \rightarrow \omega = \Pi^{-1}\mathbf{x} = (\theta(r), \phi)$ , where  $\theta(r) = 2 \tan^{-1}(r/2)$ .
- Define the **action** of the stereographic projection operator **on functions** on the plane and sphere. Consider the space of square integrable functions in  $L^2(\mathbb{R}^2, d^2\mathbf{x})$  on the plane and  $L^2(\mathbb{S}^2, d\Omega(\omega))$  on the sphere.

- The action of the **stereographic projection operator**

$\Pi : s \in L^2(\mathbb{S}^2, d\Omega(\omega)) \rightarrow p = \Pi s \in L^2(\mathbb{R}^2, d^2\mathbf{x})$  on functions is defined as

$$p(r, \phi) = (\Pi s)(r, \phi) = (1 + r^2/4)^{-1} s(\theta(r), \phi) .$$

- The **inverse stereographic projection operator**

$\Pi^{-1} : p \in L^2(\mathbb{R}^2, d^2\mathbf{x}) \rightarrow s = \Pi^{-1} p \in L^2(\mathbb{S}^2, d\Omega(\omega))$  on functions is then

$$s(\theta, \phi) = (\Pi^{-1} p)(\theta, \phi) = [1 + \tan^2(\theta/2)] p(r(\theta), \phi) .$$

# Methodology I: Dilation

- The spherical **dilation operator**  $\mathcal{D}(a, b) : s(\omega) \rightarrow [\mathcal{D}(a, b)s](\omega)$  in  $L^2(\mathbb{S}^2, d\Omega(\omega))$  is **defined as the conjugation by  $\Pi$  of the Euclidean dilation  $d(a, b)$  in  $L^2(\mathbb{R}^2, d^2\mathbf{x})$  on tangent plane at north pole**:

$$\mathcal{D}(a, b) \equiv \Pi^{-1} d(a, b) \Pi ,$$

where  $d(a, b)$  is the anisotropic Euclidean dilation operator.

- Spherical **dilation given by**

$$[\mathcal{D}(a, b)s](\omega) = [\lambda(a, b, \theta, \phi)]^{1/2} s(\omega_{1/a, 1/b}) ,$$

where  $\omega_{a,b} = (\theta_{a,b}, \phi_{a,b})$ ,  $\tan(\theta_{a,b}/2) = \tan(\theta/2) \sqrt{a^2 \cos^2 \phi + b^2 \sin^2 \phi}$  and  $\tan(\phi_{a,b}) = \frac{b}{a} \tan(\phi)$ .

- For the case where  $a = b$  the anisotropic dilation reduces to the usual isotropic case defined by  $\tan(\theta_a/2) = a \tan(\theta/2)$  and  $\phi_a = \phi$ .
- Cocycle of an anisotropic spherical dilation is defined by

$$\lambda(a, b, \theta, \phi) \equiv \frac{4a^3 b^3}{(A_- \cos \theta + A_+)^2} ,$$

where

$$A_{\pm} = a^2 b^2 \pm a^2 \sin^2 \phi \pm b^2 \cos^2 \phi .$$

For the case where  $a = b$  the anisotropic cocycle reduces to the usual isotropic cocycle.

- Although **anisotropic dilations of practical use, not wavelets** strictly speaking. In the anisotropic setting a bounded admissibility integral cannot be determined (even in the plane), thus the synthesis of a signal from its coefficients cannot be performed. **For perfect reconstruction require  $a = b$ .**

# Methodology I: Analysis

- Construct wavelet basis from affine transformation (dilation, translation) on the sphere of a mother wavelet
- The natural **extension of translations to the sphere are rotations**. Characterised by the elements of the rotation group  $SO(3)$ , which parameterise in terms of the three Euler angles  $\rho = (\alpha, \beta, \gamma)$ . Rotation of a function  $f$  on the sphere is defined by

$$[\mathcal{R}(\rho)f](\omega) = f(\rho^{-1}\omega), \quad \rho \in SO(3).$$

- **Wavelet basis** on the sphere may now be constructed from rotations and isotropic dilations (where  $a = b$ ) of a mother spherical wavelet  $\Phi \in L^2(\mathbb{S}^2, d\Omega(\omega))$ . The corresponding wavelet family  $\{\Phi_{a,\rho} \equiv \mathcal{R}(\rho)\mathcal{D}(a,a)\Phi : \rho \in SO(3), a \in \mathbb{R}_*^+\}$  provides an over-complete set of functions in  $L^2(\mathbb{S}^2, d\Omega(\omega))$ .
- The **CSWT<sub>1</sub>** of  $f \in L^2(\mathbb{S}^2, d\Omega(\omega))$  is given by the projection on to each wavelet basis function in the usual manner:

$$\widehat{\mathcal{W}}_{\Phi}^f(a, \rho) \equiv \int_{\mathbb{S}^2} d\Omega(\omega) f(\omega) \Phi_{a,\rho}^*(\omega),$$

where  $d\Omega(\omega) = \sin \theta d\theta d\phi$  is the usual invariant measure on the sphere.

- Transform general in the sense that all orientations in the rotation group  $SO(3)$  are considered, thus **directional structure is naturally incorporated**. (However, only *local* directions make any sense on  $\mathbb{S}^2$ .)

# Methodology I: Synthesis

- The **synthesis** of a signal on the sphere from its wavelet coefficients is given by

$$f(\omega) = \int_{\text{SO}(3)} d\varrho(\rho) \int_0^\infty \frac{da}{a^3} \widehat{\mathcal{W}}_\Phi^f(a, \rho) [\mathcal{R}(\rho) \widehat{L}_\Phi \Phi_a](\omega),$$

where  $d\varrho(\rho) = \sin \beta d\alpha d\beta d\gamma$  is the invariant measure on the rotation group  $\text{SO}(3)$ .

- The  $\widehat{L}_\Phi$  operator in  $L^2(\mathbb{S}^2, d\Omega(\omega))$  is defined by the action

$$(\widehat{L}_\Phi g)_{\ell m} \equiv g_{\ell m} / \widehat{C}_\Phi^\ell$$

on the spherical harmonic coefficients of functions  $g \in L^2(\mathbb{S}^2, d\Omega(\omega))$ .

- In order to ensure the perfect reconstruction of a signal synthesised from its wavelet coefficients, one requires the **admissibility condition**

$$0 < \widehat{C}_\Phi^\ell \equiv \frac{8\pi^2}{2\ell + 1} \sum_{m=-\ell}^{\ell} \int_0^\infty \frac{da}{a^3} |(\Phi_a)_{\ell m}|^2 < \infty$$

to hold for all  $\ell \in \mathbb{N}$ , where  $(\Phi_a)_{\ell m}$  are the spherical harmonic coefficients of  $\Phi_a(\omega)$ .

# Methodology I: Mother wavelets

- **Correspondence principle** between spherical and Euclidean wavelets states that the inverse stereographic projection of an *admissible* wavelet on the plane yields an *admissible* wavelet on the sphere. (Proved by [20].)
- **Mother wavelets on sphere** constructed from the projection of mother Euclidean wavelets defined on the plane:

$$\Phi(\omega) = [\Pi^{-1}\Phi_{\mathbb{R}^2}](\omega),$$

where  $\Phi_{\mathbb{R}^2} \in L^2(\mathbb{R}^2, d^2x)$  is an admissible wavelet in the plane.

- **Directional wavelets on sphere** may be naturally constructed in this setting – they are simply the projection of directional Euclidean planar wavelets on to the sphere.

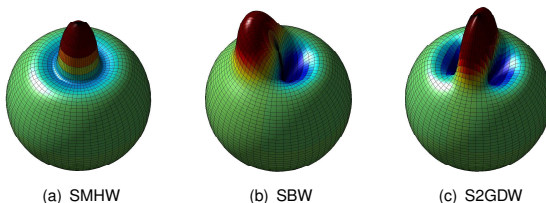


Figure: Spherical wavelets at scale  $a = b = 0.2$ .

# Methodology II: Overview

- Dilation operator defined through **association with plane** by AV98
- **Alternative idea for dilation** operator proposed by SHLA06
  - Dilation defined by scaling in harmonic space
  - But wavelet framework not directional
- **Integrated** directional approach from AV98 with harmonic scaling idea of SHLA06 (MHL06)
  - Defined directly on sphere
  - Directional structure naturally incorporated

# Methodology II: Analysis

- Dilated wavelet  $\Psi(\omega; a)$  is **defined in harmonic space** by

$$\Psi_{\ell m}(a) = \sqrt{\frac{2\ell + 1}{8\pi^2}} \Upsilon_m(\ell a),$$

where  $\Psi_{\ell m}(a)$  are the spherical harmonic coefficients of  $\Psi(\omega; a)$ ,  $\Upsilon_m(q)$  are the family of wavelet generating functions and  $a \in \mathbb{R}_*^+$  is the real, strictly positive isotropic dilation parameter. The notation adopted to represent a dilation in this setting differs to that used previously in order to reflect the different definition of the dilation operator.

- The **wavelet generating functions** are not defined on the sphere but rather on the non-negative real line:  $\Upsilon_m \in L^2(\mathbb{R}^+, dx)$ ,  $m \in \mathbb{Z}$  (although we consider only  $|m| < \ell$  for  $\Psi_{\ell m}(a)$ , one is in general free to define  $\Upsilon_m, \forall m \in \mathbb{Z}$ ).
- An overcomplete **wavelet basis** on the sphere may be constructed from the following spherical wavelet family:

$$\{[\mathcal{R}(\rho)\Psi](\omega; a) : \rho \in \text{SO}(3), a \in \mathbb{R}_*^+\}.$$

- The **CSWT<sub>II</sub>** of  $f \in L^2(\mathbb{S}^2, d\Omega(\omega))$  is given by the projection on to each wavelet basis function in the usual manner:

$$\widetilde{\mathcal{W}}_{\Upsilon}^f(a, \rho) \equiv \int_{\mathbb{S}^2} d\Omega(\omega) f(\omega) [\mathcal{R}(\rho)\Psi]^*(\omega; a).$$

- Notice that the **analysis formula** for a given dilation is **identical** to the analysis formula (4) of the CSWT<sub>I</sub>. The transform is again general in the sense that all orientations in the rotation group  $\text{SO}(3)$  are considered, thus **directional structure is naturally incorporated**.



# Methodology II: Synthesis

- To classify as wavelet analysis, **must be possible to reconstruct perfectly** the original function from its wavelet coefficients.
- The **synthesis** of a signal from its wavelet coefficients is given by

$$f(\omega) = \int_0^\infty \frac{da}{a} \int_{\text{SO}(3)} d\rho(\rho) \widetilde{W}_\Upsilon^f(a, \rho) [\mathcal{R}(\rho) \widetilde{L}_\Upsilon \Psi](\omega; a).$$

- The  $\widetilde{L}_\Upsilon$  operator in  $L^2(\mathbb{S}^2, d\Omega(\omega))$  is defined by the action

$$(\widetilde{L}_\Upsilon g)_{\ell m} \equiv g_{\ell m} / \widetilde{C}_\Upsilon^\ell$$

on the spherical harmonic coefficients of functions  $g \in L^2(\mathbb{S}^2, d\Omega(\omega))$ .

- For perfect reconstruction require the **admissibility criteria**

$$0 < \widetilde{C}_\Upsilon^\ell \equiv \frac{8\pi^2}{2\ell + 1} \sum_{m=-\ell}^{\ell} \int_0^\infty \frac{da}{a} |\Psi_{\ell m}(a)|^2 < \infty, \quad \text{to hold } \forall \ell.$$

- Relate the admissibility criteria that each spherical wavelet must satisfy to an equivalent **admissibility condition for the family of wavelet generating functions**:

$$0 < \widetilde{C}_\Upsilon^\ell = \sum_{m=-\ell}^{\ell} \int_0^\infty \frac{dq}{q} |\Upsilon_m(q)|^2 < \infty.$$

Since  $\int_0^\infty \frac{dq}{q} |\Upsilon_m(q)|^2$  is always non-negative it is possible to recast the admissibility condition on the family  $\Upsilon_m$  in the following form:  $\int_0^\infty \frac{dq}{q} |\Upsilon_m(q)|^2 < \infty, \forall m \in \mathbb{Z}$  and  $\exists m \in \mathbb{Z}$  such that  $\int_0^\infty \frac{dq}{q} |\Upsilon_m(q)|^2 \neq 0$ .

# Methodology II: Mother wavelets

- Wavelets on the sphere may be constructed in harmonic space from the **analogue of the Fourier definition** of planar Euclidean wavelets. Must then check that the candidate wavelets are admissible.
- Construct the spherical analogue of the Morlet wavelet** using our spherical wavelet formalism.
  - Differs to the definition of the spherical Morlet wavelet constructed from the projection of the planar Morlet wavelet on to the sphere.
  - The planar Morlet wavelet is defined by a Gaussian in Fourier space centred on the wave vector of the wavelet, hence we define the analogue of the Morlet wavelet on the sphere by a Gaussian in spherical harmonic space.
  - Various associations between Fourier and spherical harmonic space are possible. Here we choose to associate  $\ell$  and  $m$  in spherical harmonic space with the  $x$  and  $y$  components of a vector in Fourier space respectively.
  - The wavelet generating functions are defined by

$$\Upsilon_m(\ell a) = e^{-\frac{(\ell a - L)^2 + (m - M)^2}{2}} - e^{-\frac{(\ell a)^2 + L^2 + (m - M)^2}{2}},$$

where  $L \in \mathbb{N}$  and  $M \in \mathbb{Z}$ ,  $|M| < L$  define the centre of the Gaussian when  $a = 1$ . The correction term subtracted is included to ensure admissibility.

- Before proceeding it is necessary to check that the candidate wavelet generating functions generate admissible spherical wavelets. It has been shown that the admissibility integral for the wavelet generating functions converges (see MHL06 [10]).

# Methodology II: Mother wavelets

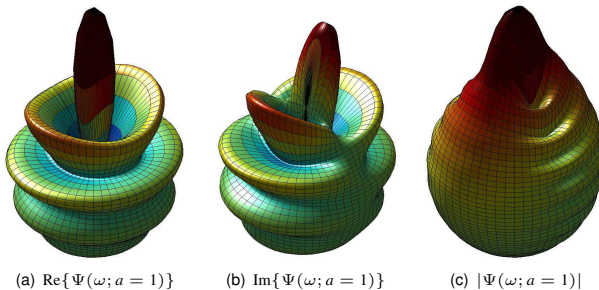


Figure: Plots of the analogue of the Morlet wavelet constructed on the sphere for  $a = 1$ .

# Methodology II: Mother wavelets

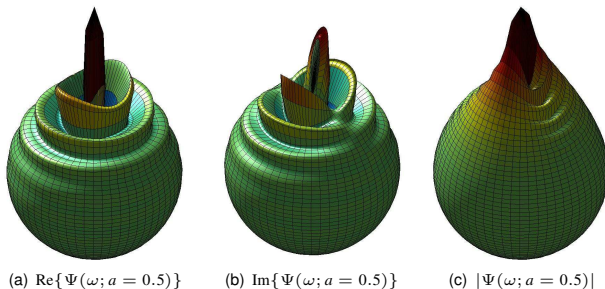


Figure: Plots of the analogue of the Morlet wavelet constructed on the sphere for  $a = 0.5$ .

# Comparison

- **Methodology I:**
  - Defined in real space easily but not harmonic space
  - Suitable for generic analyses plus problems posed naturally in real space
- **Methodology II:**
  - Defined in harmonic space easily but not real space
  - Suitable for generic analyses plus problems posed naturally in harmonic space
  - All functions and operators defined directly on the sphere
  - Remains to be seen if leads to further practical advantages, *e.g.* localisation properties (focus of further research)

# Fast algorithms

- Direct analysis **computationally infeasible** for large data sets, such as WMAP ( $\sim 3$  megapixels) and Planck ( $\sim 50$  megapixels)
- **Fast algorithms essential** (for a review see [22])
  - Factoring of rotations: McEwen *et al.* 2007 [11]
  - Separation of variables: Wiaux *et al.* 2005 [21]
- Renders analysis **computationally affordable**
- Both methodologies have the same analysis formula for a given dilation  
 $\Rightarrow$  fast algorithms **applicable to both methodologies**

# Outline

- 1 Motivation
- 2 Wavelets on the sphere
  - History
  - Methodology I
  - Methodology II
  - Comparison
  - Fast algorithms
- 3 Wavelet steerability**
  - **Steerability**
  - **Morphological measures**
- 4 Detecting the ISW effect
  - Background
  - Procedures
  - Data and simulations
  - Detections

# Wavelet steerability

- Defined on the sphere by Wiaux *et al.* (2005) [20]
- For steerable wavelets, wavelet for any orientation  $\gamma$  given by weighted sum of basis wavelets:

$$\psi_{\gamma}(\omega) = \sum_{m=1}^M k_m(\gamma) \psi_m(\omega)$$

- Due to linearity of the wavelet transform, property extends to wavelet coefficients.



# Wavelet steerability

- Defined on the sphere by Wiaux *et al.* (2005) [20]
- For steerable wavelets, wavelet for any orientation  $\gamma$  given by weighted sum of basis wavelets:

$$\psi_{\gamma}(\omega) = \sum_{m=1}^M k_m(\gamma) \psi_m(\omega)$$

- Due to linearity of the wavelet transform, property extends to wavelet coefficients.

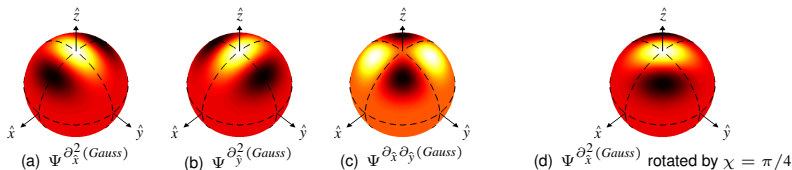


**Figure:** Second Gaussian derivative wavelet on the sphere for  $a = 0.4$ . Dark and light regions respectively identify negative and positive values. The rotated wavelet illustrated in panel (d) can be constructed from a sum of weighted versions of the basis wavelets illustrated in panels (a) through (c). (Illustrations reproduced from [20].)

# Wavelet steerability

- Defined on the sphere by Wiaux *et al.* (2005) [20]
- For steerable wavelets, wavelet for any orientation  $\gamma$  given by weighted sum of basis wavelets:

$$\psi_{\gamma}(\omega) = \sum_{m=1}^M k_m(\gamma) \psi_m(\omega)$$

- Due to linearity of the wavelet transform, property extends to wavelet coefficients.

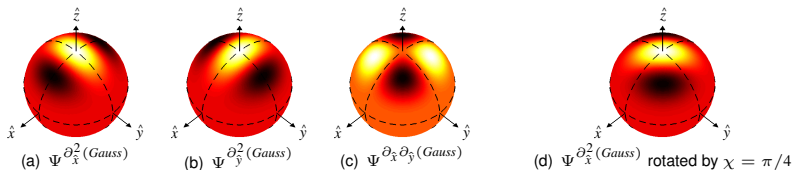


**Figure:** Second Gaussian derivative wavelet on the sphere for  $a = 0.4$ . Dark and light regions respectively identify negative and positive values. The rotated wavelet illustrated in panel (d) can be constructed from a sum of weighted versions of the basis wavelets illustrated in panels (a) through (c). (Illustrations reproduced from [20].)

# Morphological measures

- Steerability may be used to **compute measures of the morphology of local features**.
  - **Orientation**  $D(\omega, a)$ : Orientation of feature of maximum wavelet coefficient at each position on the sphere
  - **Signed-intensity**  $I(\omega, a)$ : Maximum wavelet coefficient at given orientation
  - **Elongation**  $E(\omega, a)$ : Unity minus ratio of wavelet coefficient in orthogonal direction relative to maximum wavelet coefficient

# Morphological measures

- Steerability may be used to **compute measures of the morphology of local features**.
  - Orientation**  $D(\omega, a)$ : Orientation of feature of maximum wavelet coefficient at each position on the sphere
  - Signed-intensity**  $I(\omega, a)$ : Maximum wavelet coefficient at given orientation
  - Elongation**  $E(\omega, a)$ : Unity minus ratio of wavelet coefficient in orthogonal direction relative to maximum wavelet coefficient

ILC signed-intensity

ILC orientation

ILC elongation

(a) Signed-intensity

(b) Orientation

(c) Elongation

**Figure:** Morphological measures of the WMAP ILC map for scales 50–600 arcmin.

# Outline

- 1 Motivation
- 2 Wavelets on the sphere
  - History
  - Methodology I
  - Methodology II
  - Comparison
  - Fast algorithms
- 3 Wavelet steerability
  - Steerability
  - Morphological measures
- 4 **Detecting the ISW effect**
  - **Background**
  - **Procedures**
  - **Data and simulations**
  - **Detections**

# ISW effect

- Late **ISW effect**
  - CMB photons blue (red) shifted when fall into (out of) potential wells
  - Evolution of potential during photon propagation  
→ net change in photon energy
  - Gravitation potentials constant w.r.t. conformal time in matter dominated universe
  - Deviation from matter domination due to curvature or dark energy causes potentials to evolve with time  
→ secondary anisotropy induced in CMB
- WMAP shown universe is (nearly) flat  
detection of ISW effect → direct **evidence for dark energy**
- Cannot isolate the ISW signal from CMB anisotropies easily
- Instead, **detect by cross-correlating** CMB anisotropies with tracers of large scale structure (Crittenden & Turok 1996 [5])
- Previous works
  - Real space angular correlation function  
(e.g. Boughn & Crittenden 2002, 2004 [4, 3])
  - Harmonic space cross-angular power spectrum  
(e.g. Afshordi *et al.* 2004 [1])
  - Wavelet correlation (Vielva *et al.* 2005 [19]; McEwen 2006 *et al.* [12])
- Search for correlation between **morphological measures** of local features

# Procedures

- Work done with Yves Wiaux, Pierre Vanderghenst, Mike Hobson & Anthony Lasenby [13].
- **Correlate morphological measures** of signed-intensity, orientation and elongation through a steerable wavelet analysis with the second Gaussian derivative wavelet (S2GDW):

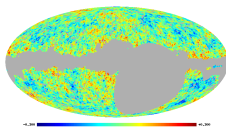
$$X_{S_i}^{\text{NT}}(a) = \frac{1}{N_p} \sum_{\omega_0} S_i^{\text{N}}(\omega_0, a) S_i^{\text{T}}(\omega_0, a),$$

where  $S_i = \{\mathcal{W}, I, D, E\}$ .

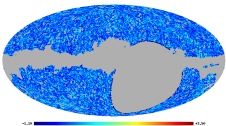
- Two procedures proposed:
  - **Local morphological correlation**
  - **Matched intensity correlation**
- In absence of ISW effect don't expect to observe a significant correlation in any of these measures
- Compute correlation of morphological measures from WMAP and NVSS and compare to Monte Carlo simulations to determine significance of any candidate detections.

# Data and simulations

- **WMAP** three-year and **NVSS** radio galaxy data
- Perform 1000 **Monte Carlo simulations** to quantify significance of any detections of correlation
- Check data sensitive to morphological measures proposed



(a) WMAP



(b) NVSS

**Figure:** WMAP co-added three-year and NVSS maps after application of the joint mask. The maps are downsampled to a pixel size of  $\sim 55'$ .



# Data and simulations

- **WMAP** three-year and **NVSS** radio galaxy data
- Perform 1000 **Monte Carlo simulations** to quantify significance of any detections of correlation
- Check data sensitive to morphological measures proposed

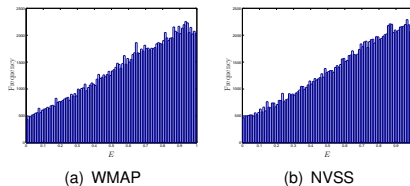
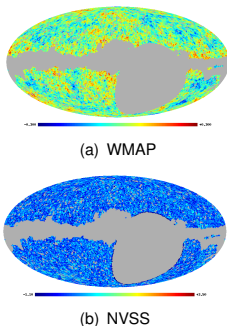


**Figure:** Histograms of the elongation values computed from the WMAP and NVSS data for all scales. Many elongation values lie far from zero, thereby justifying the morphological analyses proposed.

**Figure:** WMAP co-added three-year and NVSS maps after application of the joint mask. The maps are downsampled to a pixel size of  $\sim 55'$ .

# Detections: Local morphological correlation

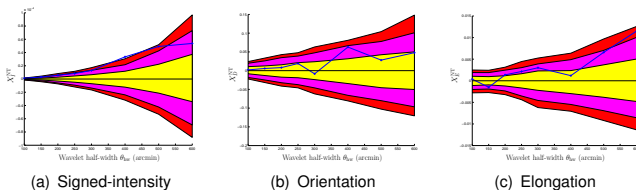


**Figure:** Correlation statistics computed for each morphological measure in the local morphological analysis, from the WMAP co-added map and the NVSS map. Significance levels obtained from the 1000 Monte Carlo simulations are shown by the shaded regions for 68% (yellow), 95% (magenta) and 99% (red) levels.

- $\chi^2$  test performed to compute significance of detections when all scales considered in aggregate
  - Signed-intensity: detection at 95% significance
  - Orientation: detection at 93% significance
  - Elongation: detection at 85% significance
- Foreground contamination and instrumental systematics ruled out as source of the correlation

# Detections: Matched intensity correlation

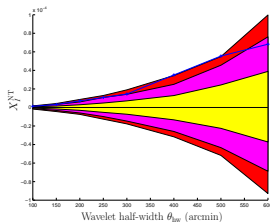


**Figure:** Correlation statistics computed for signed-intensity in the matched intensity analysis, from the WMAP co-added map and the NVSS map. Significance levels obtained from the 1000 Monte Carlo simulations are shown by the shaded regions for 68% (yellow), 95% (magenta) and 99% (red) levels.

- $\chi^2$  test performed to compute significance of detection when all scales considered in aggregate
  - Signed-intensity: detection at **99.9% significance**
- Foreground contamination and instrumental systematics ruled out as source of the correlation

# Correlation by eye?

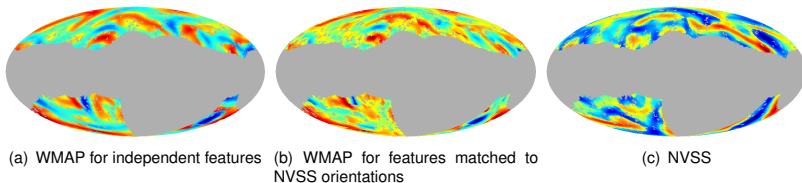


**Figure:** Morphological signed-intensity maps corresponding to the scale ( $a = 400'$ ) on which the maximum detections of correlation are made. In panel (a) signed-intensities are shown for local features extracted independently from the WMAP co-added data, whereas in panel (b) signed-intensities are shown for local features in the WMAP co-added data that are matched in orientation to local features in the NVSS data. Due to the strength of the correlation in the data, it is possible to observe the correlation both between maps (a) and (c) and between maps (b) and (c) by eye.

# Summary and future work

- Wavelets on the sphere
  - **Powerful** signal analysis tool
  - **New methodology**  
Directional and all operators and functions defined on sphere directly  
Future work: examine localisation properties; discretise and implement synthesis
  - **Steerable wavelets**  
Allows infinite precision in orientation  
Facilitates morphological analyses
- Detection of the ISW effect
  - Search for a **morphological correlation**
  - Detected at **99.9% significance**  $\Rightarrow$  independent verification of dark energy
  - Probes **morphological nature** of correlations
  - Future work: use correlations detected to **constrain dark energy parameters** (not trivial!)

# References I

- [1] N. Afshordi, Y.-S. Loh, and M. A. Strauss.  
Cross-correlation of the cosmic microwave background with the 2MASS galaxy survey: signatures of dark energy, hot gas, and point sources.  
*Phys. Rev. D.*, D69:083524, 2004.
- [2] J.-P. Antoine and P. Vandergheynst.  
Wavelets on the n-sphere and related manifolds.  
*J. Math. Phys.*, 39(8):3987–4008, 1998.
- [3] S. Boughn and R. Crittenden.  
A correlation of the cosmic microwave sky with large scale structure.  
*Nature*, 427:45–47, 2004.
- [4] S. P. Boughn and R. G. Crittenden.  
Cross-correlation of the cosmic microwave background with radio sources: constraints on an accelerating universe.  
*Phys. Rev. Lett.*, 88:021302, 2002.
- [5] R. G. Crittenden and N. Turok.  
Looking for  $\Lambda$  with the Rees-Sciama effect.  
*Phys. Rev. Lett.*, 76:575–578, 1996.
- [6] S. Dahlke and P. Maass.  
Continuous wavelet transforms with applications to analyzing functions on sphere.  
*J. Fourier Anal. and Appl.*, 2:379–396, 1996.
- [7] W. Freeden, T. Gervens, and M. Schreiner.  
*Constructive approximation on the sphere: with application to geomathematics.*  
Clarendon Press, Oxford, 1997.
- [8] W. Freeden and U. Windheuser.  
Combined spherical harmonic and wavelet expansion – a future concept in the Earth's gravitational determination.  
*Applied Comput. Harm. Anal.*, 4:1–37, 1997.
- [9] M. Holschneider.  
Continuous wavelet transforms on the sphere.  
*J. Math. Phys.*, 37:4156–4165, 1996.
- [10] J. D. McEwen, M. P. Hobson, and A. N. Lasenby.  
A directional continuous wavelet transform on the sphere.  
*ArXiv*, 2006.

# References II

- [11] J. D. McEwen, M. P. Hobson, D. J. Mortlock, and A. N. Lasenby.  
Fast directional continuous spherical wavelet transform algorithms.  
*IEEE Trans. Sig. Proc.*, 55(2):520–529, 2007.
- [12] J. D. McEwen, P. Vielva, M. P. Hobson, E. Martínez-González, and A. N. Lasenby.  
Detection of the ISW effect and corresponding dark energy constraints made with directional spherical wavelets.  
*Mon. Not. Roy. Astron. Soc.*, 373:1211–1226, 2007.
- [13] J. D. McEwen, Y. Wiaux, M. P. Hobson, P. Vanderghelynst, and A. N. Lasenby.  
Probing dark energy with steerable wavelets through correlation of WMAP and NVSS local morphological measures.  
*ArXiv*, 2007.
- [14] F. J. Narcowich and J. D. Ward.  
Non-stationary wavelets on the  $m$ -sphere for scattered data.  
*Applied Comput. Harm. Anal.*, 3:324–336, 1996.
- [15] D. Potts, G. Steidl, and M. Tasche.  
Kernels of spherical harmonics and spherical frames.  
In F. Fontanella, K. Jetter, and P.-J. Laurent, editors, *Advanced Topic in Multivariate Approximation*, pages 1–154, Singapore, 1996. World Scientific.
- [16] J. L. Sanz, D. Herranz, M. López-Caniego, and F. Argüeso.  
Wavelets on the sphere – application to the detection problem.  
In *EUSIPCO*, 2006.
- [17] P. Schröder and W. Sweldens.  
Spherical wavelets: efficiently representing functions on the sphere.  
In *Computer Graphics Proceedings (SIGGRAPH '95)*, pages 161–172, 1995.
- [18] B. Torrèsani.  
Position-frequency analysis for signals defined on spheres.  
*Signal Proc.*, 43:341–346, 1995.
- [19] P. Vielva, E. Martínez-González, and M. Tucci.  
Cross-correlation of the cosmic microwave background and radio galaxies in real, harmonic and wavelet spaces: detection of the integrated Sachs-Wolfe effect and dark energy constraints.  
*Mon. Not. Roy. Astron. Soc.*, 365:891–901, 2006.

# References III

- [20] Y. Wiaux, L. Jacques, and P. Vandergheynst.  
Correspondence principle between spherical and Euclidean wavelets.  
*Astrophys. J.*, 632:15–28, 2005.
- [21] Y. Wiaux, L. Jacques, P. Vielva, and P. Vandergheynst.  
Fast directional correlation on the sphere with steerable filters.  
*Astrophys. J.*, 652:820–832, 2006.
- [22] Y. Wiaux, J. D. McEwen, and P. Vielva.  
Complex data processing: fast wavelet analysis on the sphere.  
*J. Fourier Anal. and Appl.*, invited contribution, in press, 2007.